Electronic Supplementary Information

Au Atom Tailoring of Palladium Nanocatalysts to Boost Cathodically Coupling of Carbon Dioxide and Methanol into Dimethyl Carbonate

Xue-Han Guan [a, 1], Ke-An Wang [a, 1], Zhen-Long Wang [a, 1], Huan-Chuan Hu [a], Biao Feng [c], Li-Jun Yang [c], Hai-Bin Zhu [a, *], Hui Yang [b, *]

[a] *School of Chemistry and Chemical Engineering, Southeast University, 211189 Nanjing, China*

[b] *Shanghai Advanced Research Institute, Chinese Academy of Sciences, 201210 Shanghai, China*

[c] *Key Laboratory of Mesoscopic Chemistry of MOE and Jiangsu Provincial Laboratory for Nanotechnology, School of Chemistry and Chemical Engineering, Nanjing University, 210023 Nanjing, China*

[*] To whom correspondence should be addressed. E-mail: zhuhaibin@seu.edu.cn (H.-B. Zhu)

[*] To whom correspondence should be addressed. E-mail: yangh@sari.ac.cn (H. Yang)

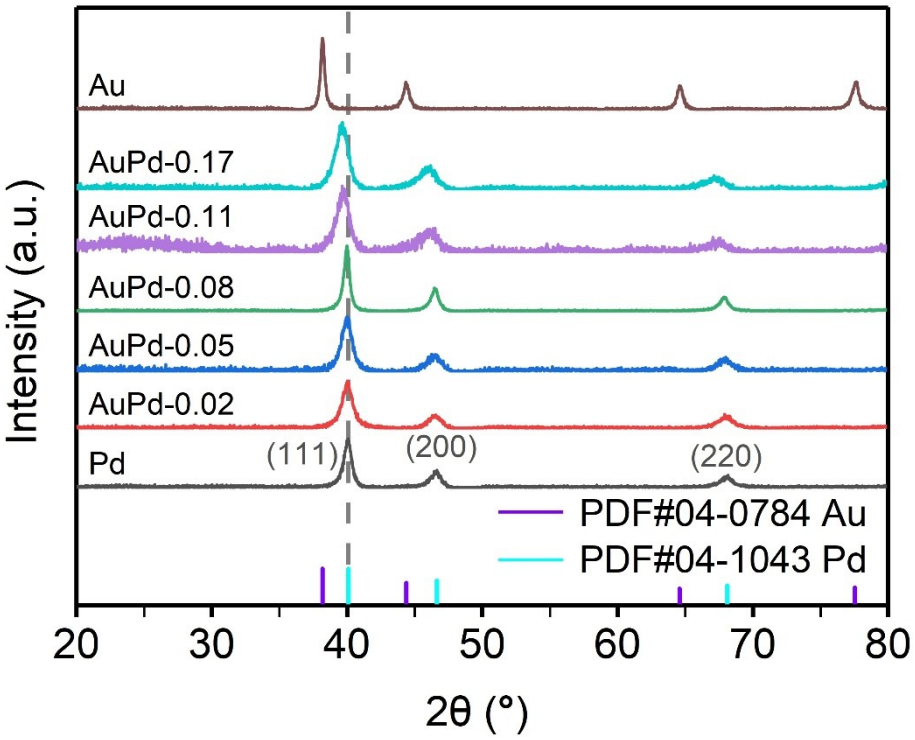

Figure S1. PXRD spectra of AuPd-x, Au NPs and Pd NPs.

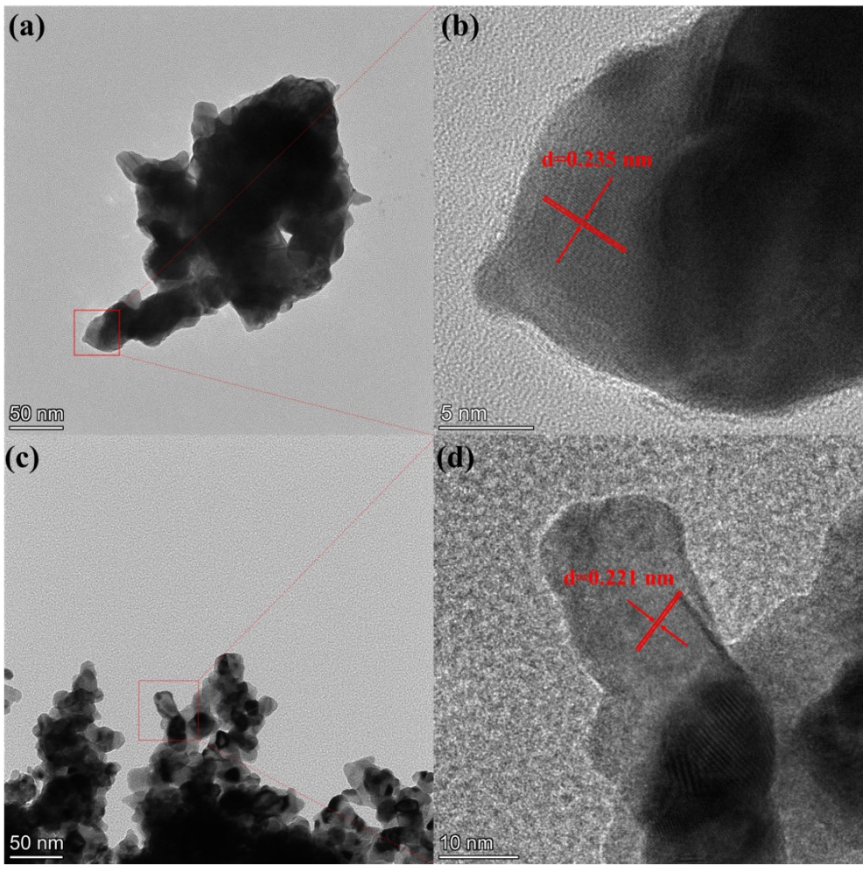

Figure S2. (a-b) TEM images of Pd NPs; (c-d) TEM images of Au NPs.

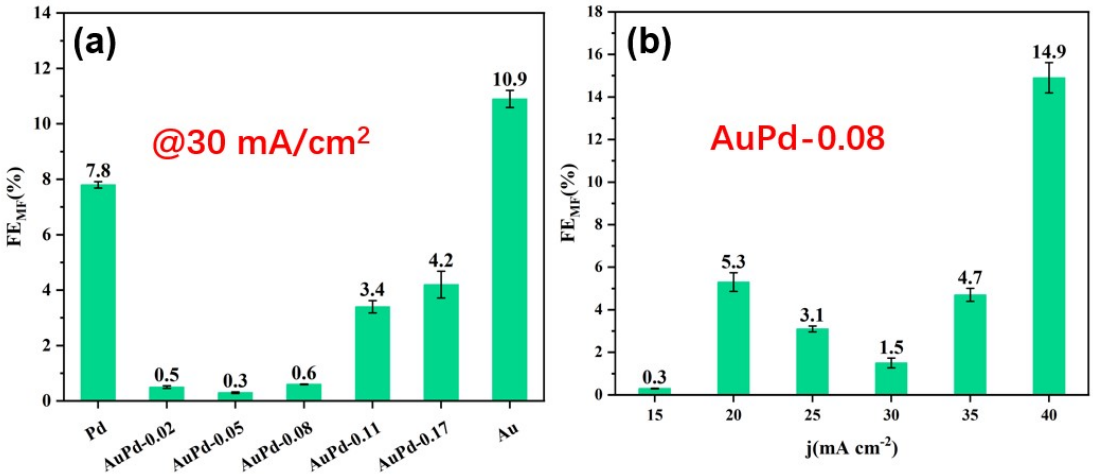

Figure S3. (a) FE of MF with AuPd-x, Pd and Au NPs at 30 mA/cm^2; (b) FE of MF with AuPd-0.08 at different current density.

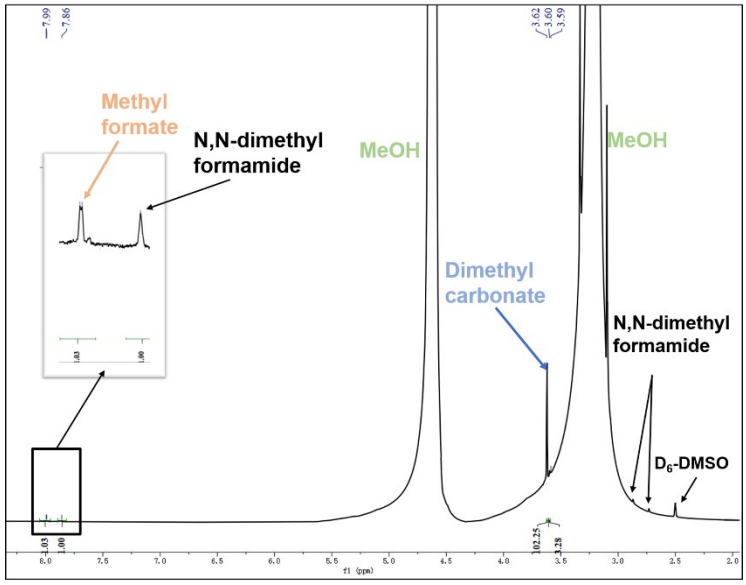

Figure S4. ^{1}H-NMR spectra of electrolyte with DMF as the internal standard.

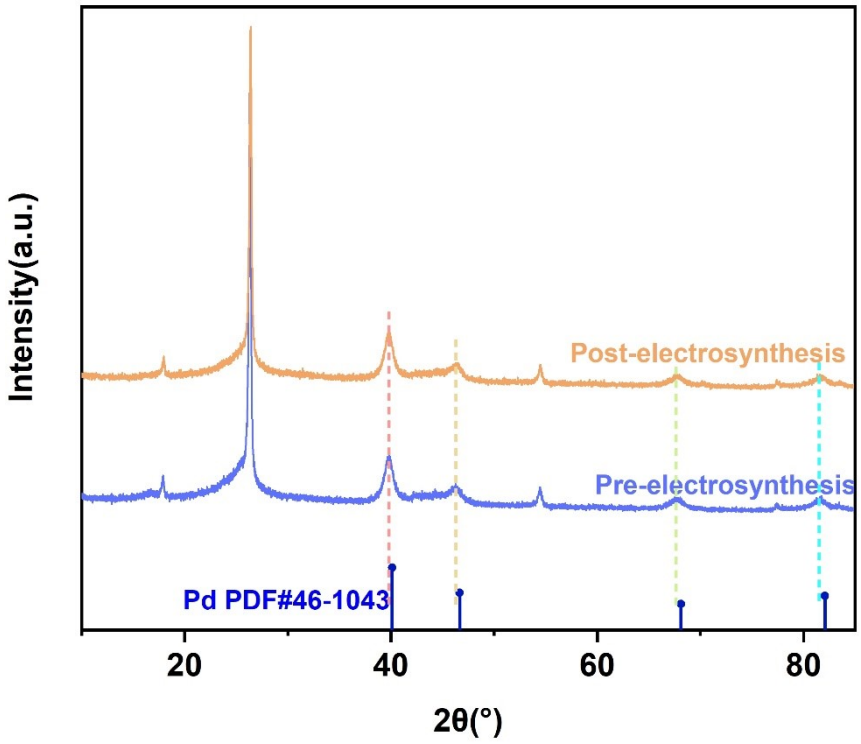

Figure S5. PXRD spectra of AuPd-0.08 loaded on carbon paper before and after electrolysis.

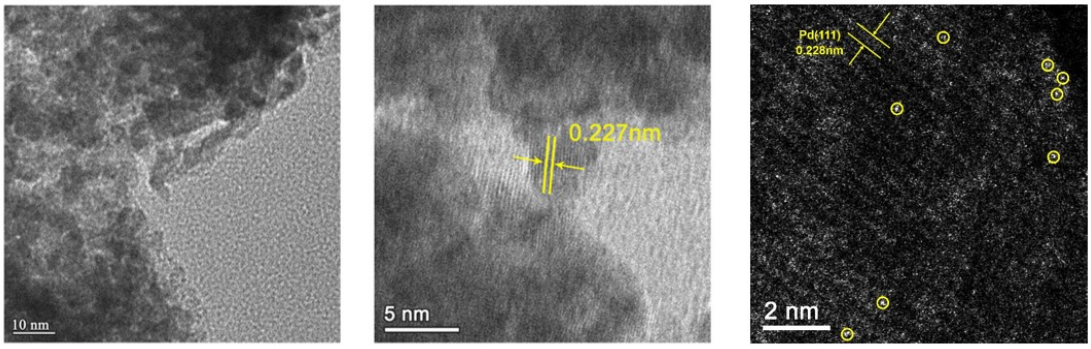

Figure S6. TEM images of AuPd-0.08 after electrolysis.

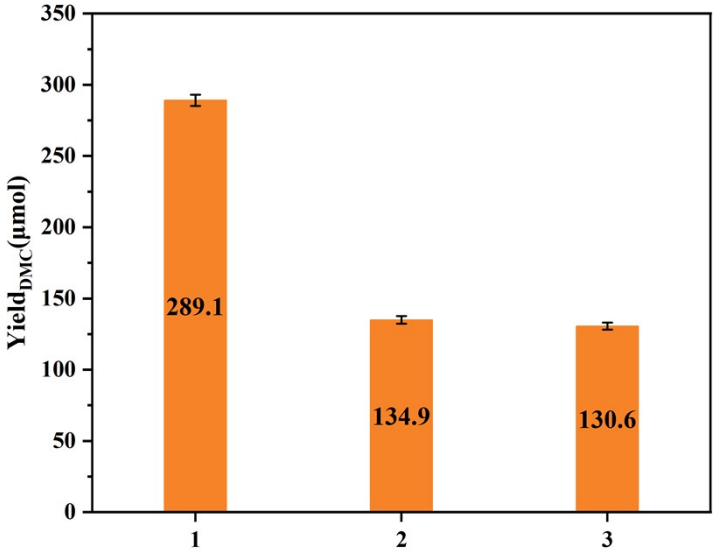

Figure S7. Evaluating the effect of the dissolved metal on DMC performance. 1: electrolysis under optimal reaction conditions for 1 hr. 2: electrolysis under optimal reaction conditions for 30 min. 3: AuPd-0.08 is used as the cathode for electrolysis for 30 minutes, and then replaced with Au foil cathode to continue electrolysis for 30 minutes.

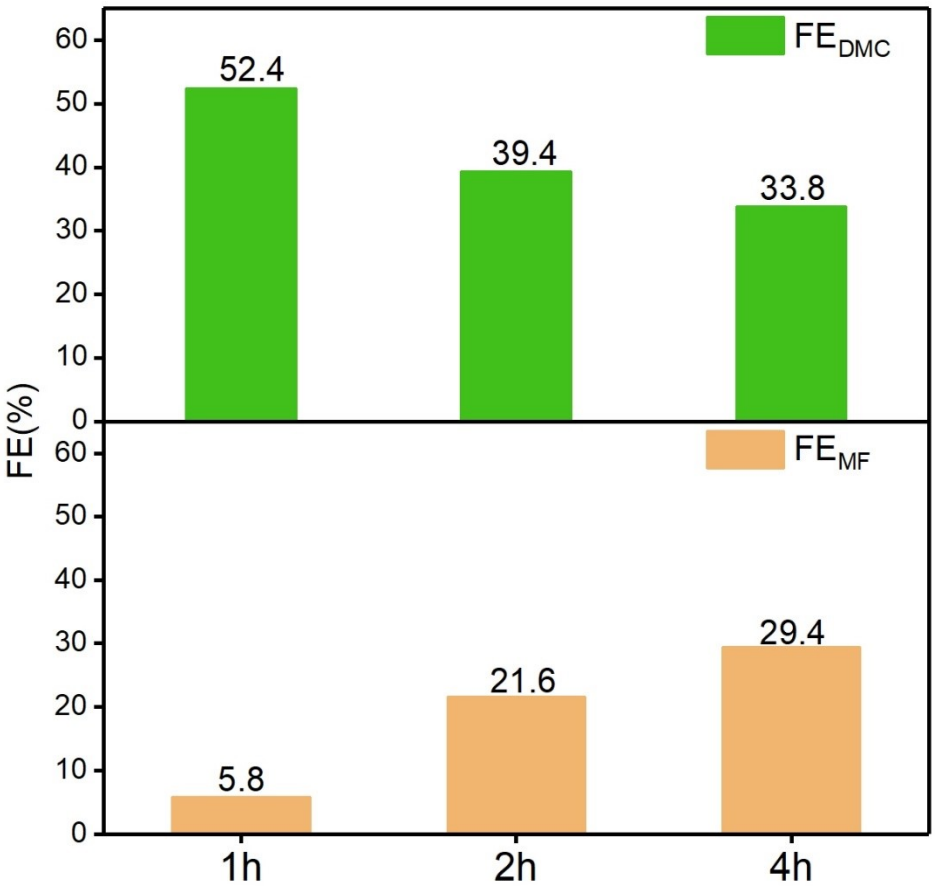

Figure S8. (a) DMC performance of AuPd-0.08 after 2 hrs and 4hrs (upper), and carbon paper stability test showing an increasing MF production with the time (lower).

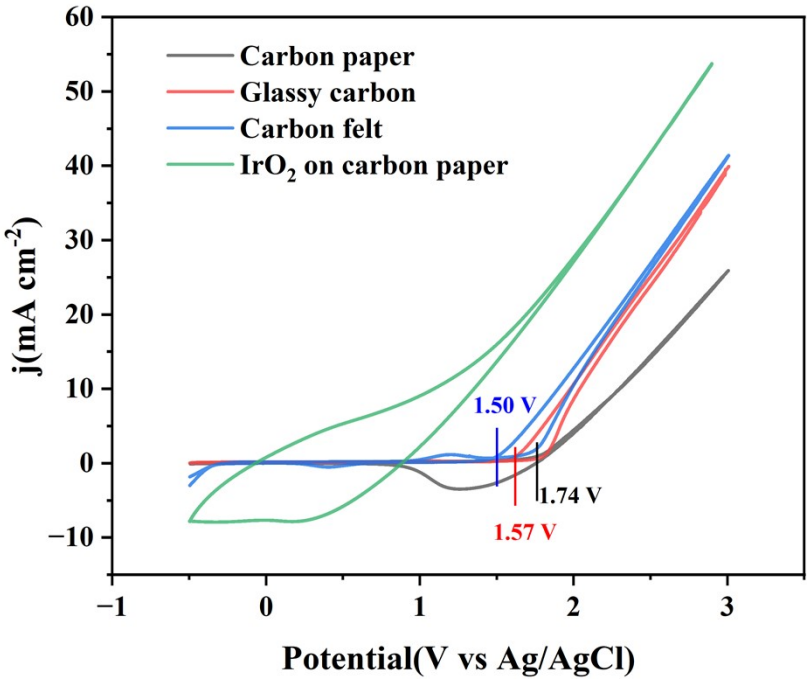

Figure S9. CV tests on different anode materials in 0.1 M $NaBF_4$ methanol solution.

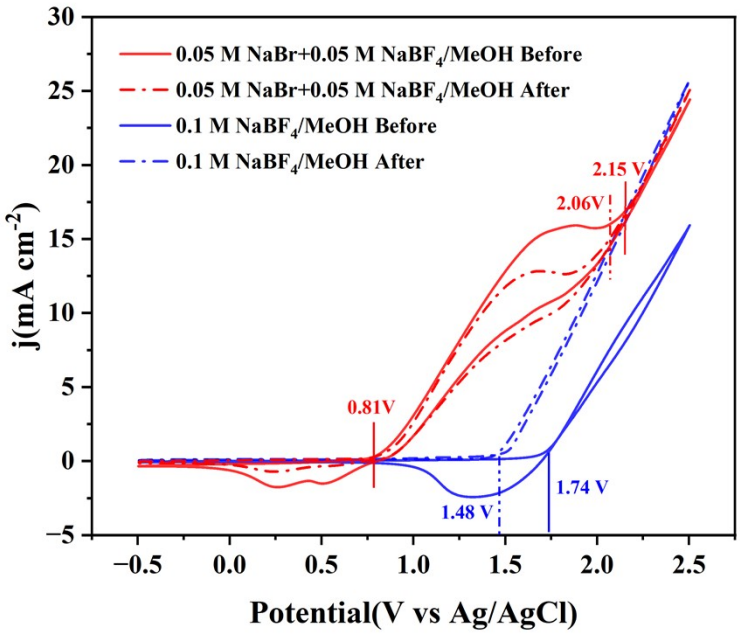

Figure S10. CV tests of CP in 0.1 M $NaBF_4$ methanol solution and 0.05 M $NaBF_4$+0.05 M NaBr methanol solution before and after 2-hr DMC electrolysis.

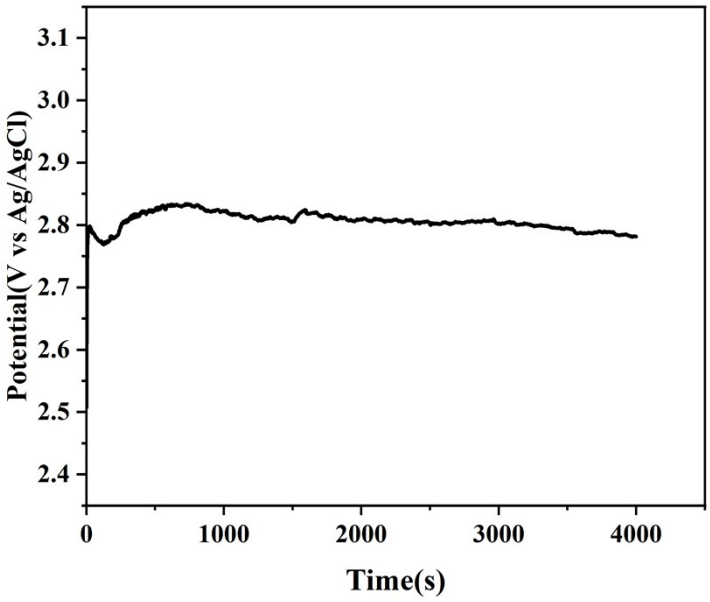

Figure S11. Monitoring the applied potential of CP anode during DMC electrosynthesis @ 30 mA/cm^2.

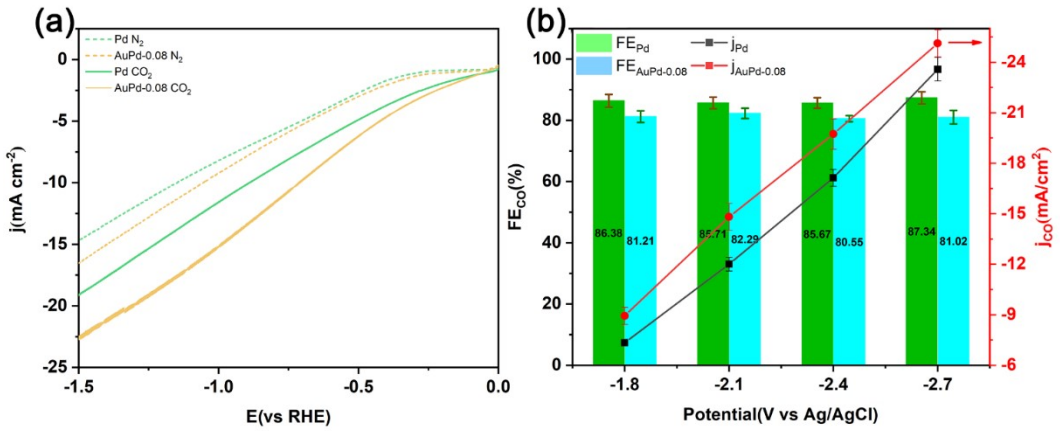

Figure S12. (a) LSV plots of Pd NPs and AuPd-0.08 under N_2 and CO_2 atmospheres. (b) Comparison of FE and partial current density of CO between Pd NPs and AuPd-0.08.

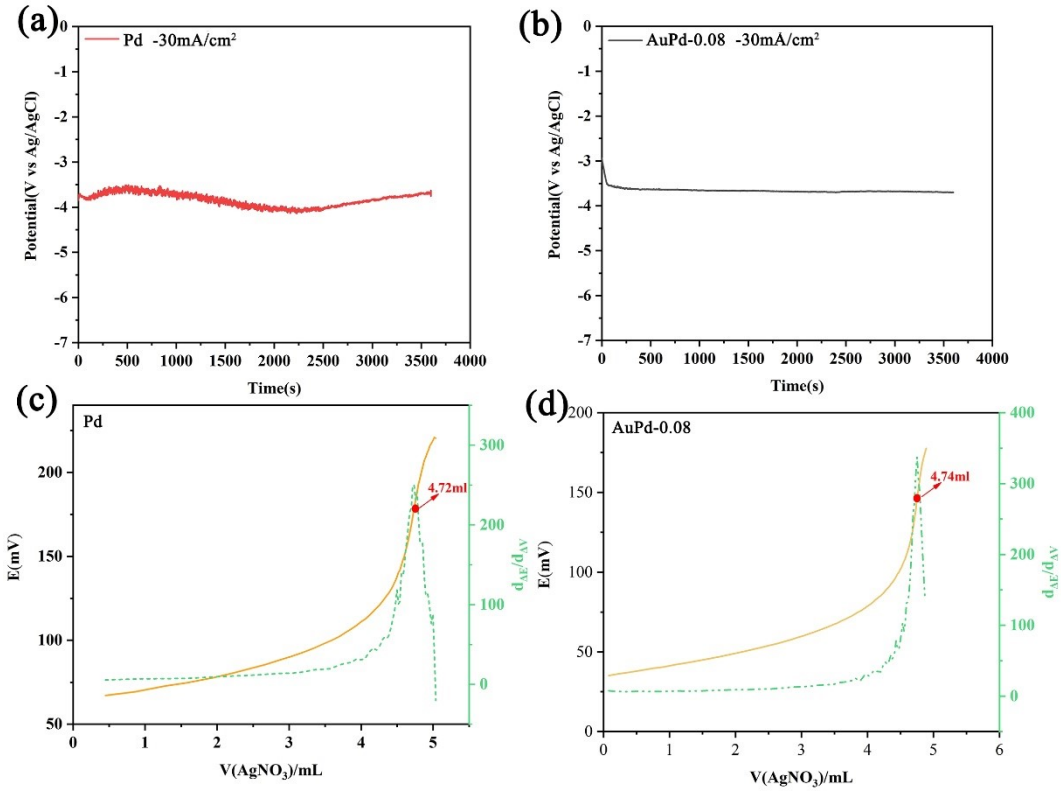

Figure S13. (a-b) Cathode potential of AuPd-0.08 and Pd NPs; (c-d) Br_2 concentration for AuPd-0.08 and Pd NPs.

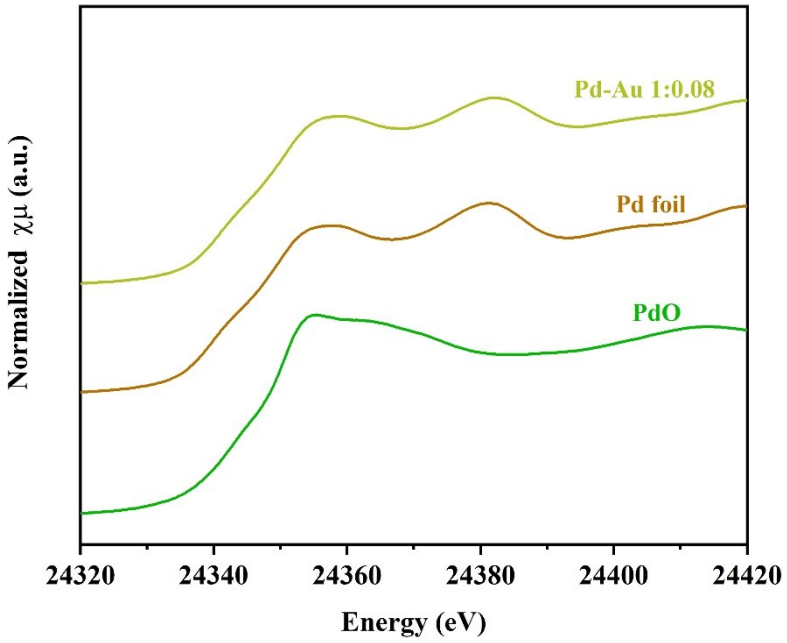

Figure S14. Pd k-edge XANES spectra of Pd foil, PdO, and AuPd-0.08.

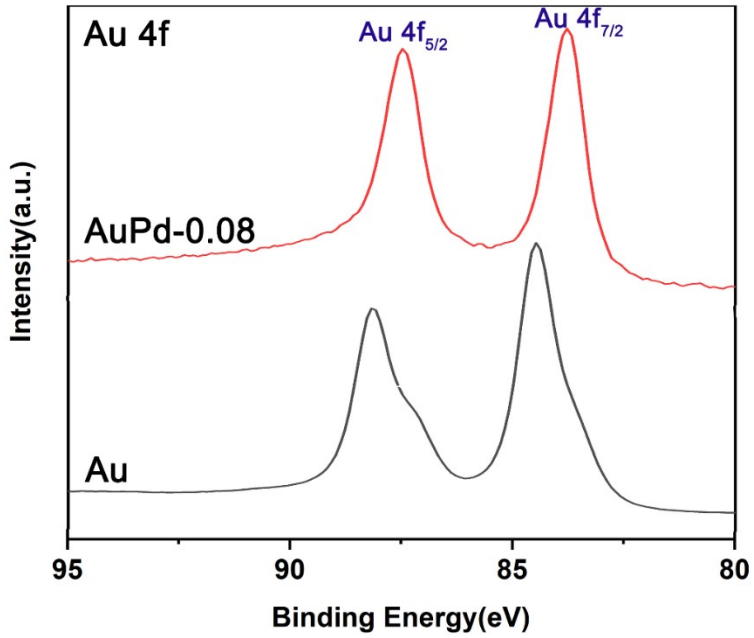

Figure S15. XPS spectra of Au 4f in AuPd-0.08 and Au.

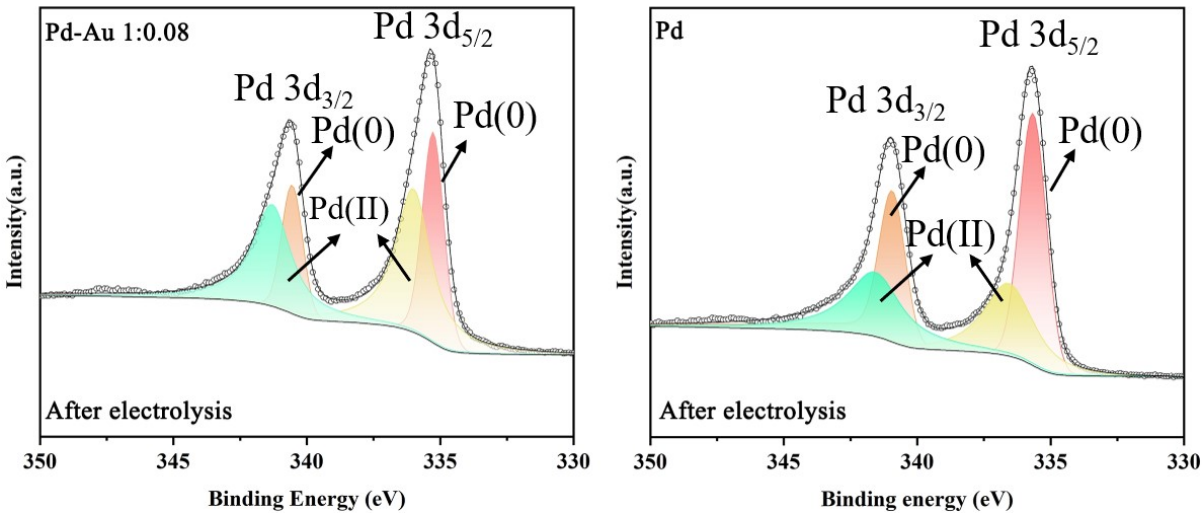

Figure S16. Pd 3d XPS spectra of (a) AuPd-0.08, and (b) Pd NPs.

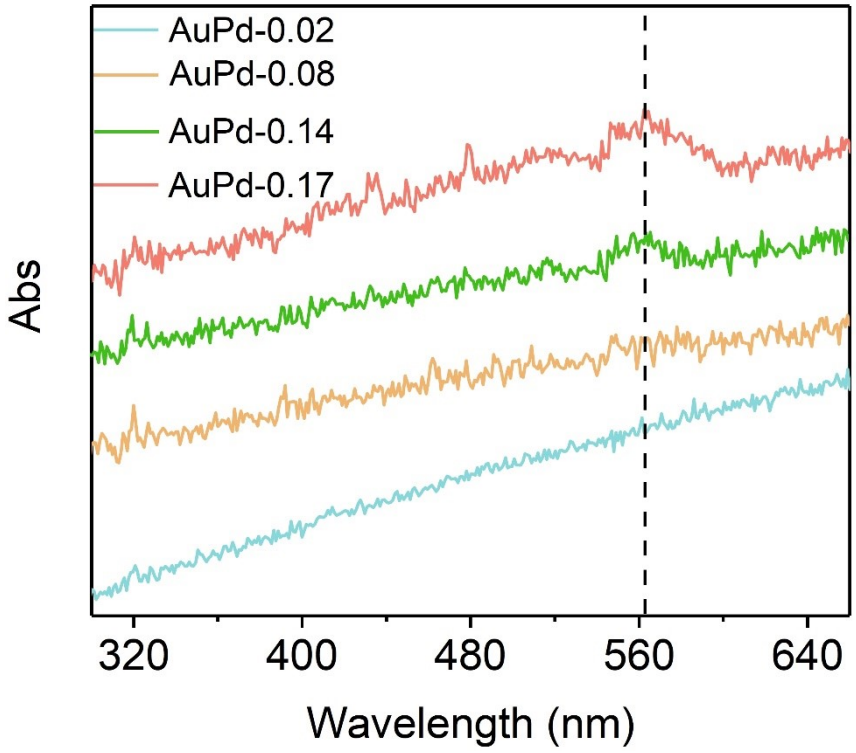

Figure S17. UV-Vis absorption spectra of AuPd-x (x = 0.02, 0.08, 0.14 and 0.17).

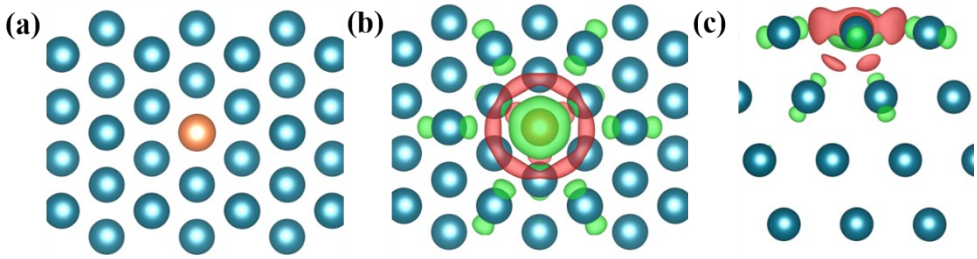

Figure S18. (a) Structure of Au single atom doped on Pd(111) surface. Orange and cyan balls represent gold and palladium, respectively. (b) and (c) are the top and side view of the charge density difference of Au single atom doped on Pd(111) surface, where green and red isosurfaces represent electron depletion and accumulation, and the isosurface unit was electrons per cubic angstrom ($e^{-}/Å^{3}$) and the levels were set as 0.0035.

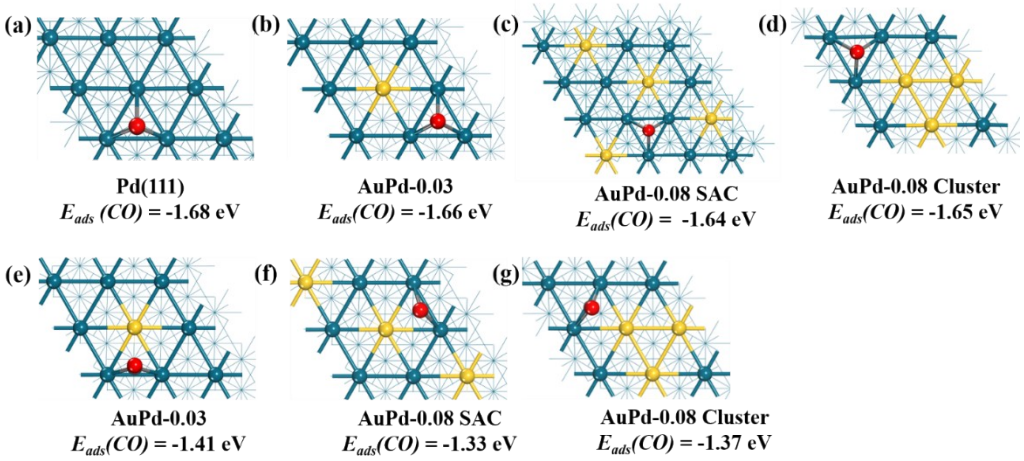

Figure S19. (a-d) Structure of Au single atom doped on Pd(111) surface. Orange and cyan balls represent gold and palladium, respectively. (e-g) Bridge adsorption configurations of CO on different doping surfaces.

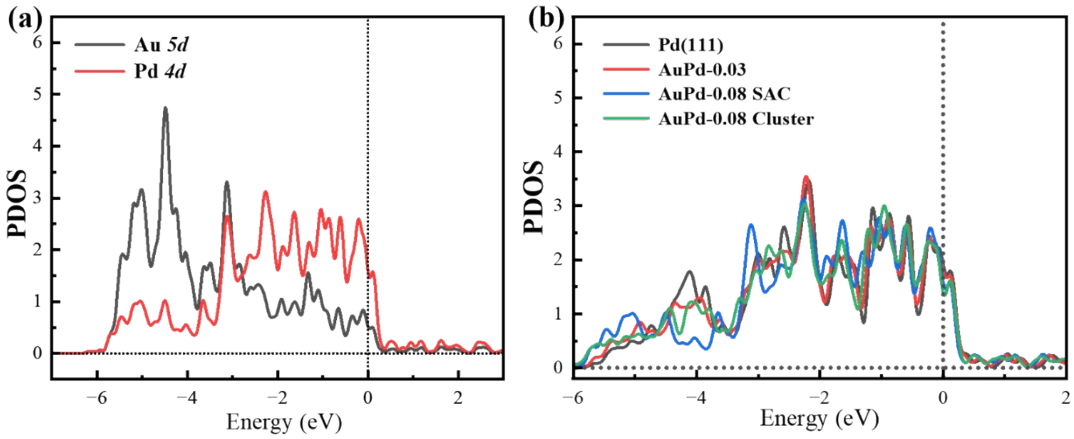

Figure S20. (a) The PDOS of d-band for AuPd-0.08 SAC. (b) The PDOS of d-band of Pd in Pd(111), AuPd-0.03, AuPd-0.08 SAC and AuPd-0.08 cluster.

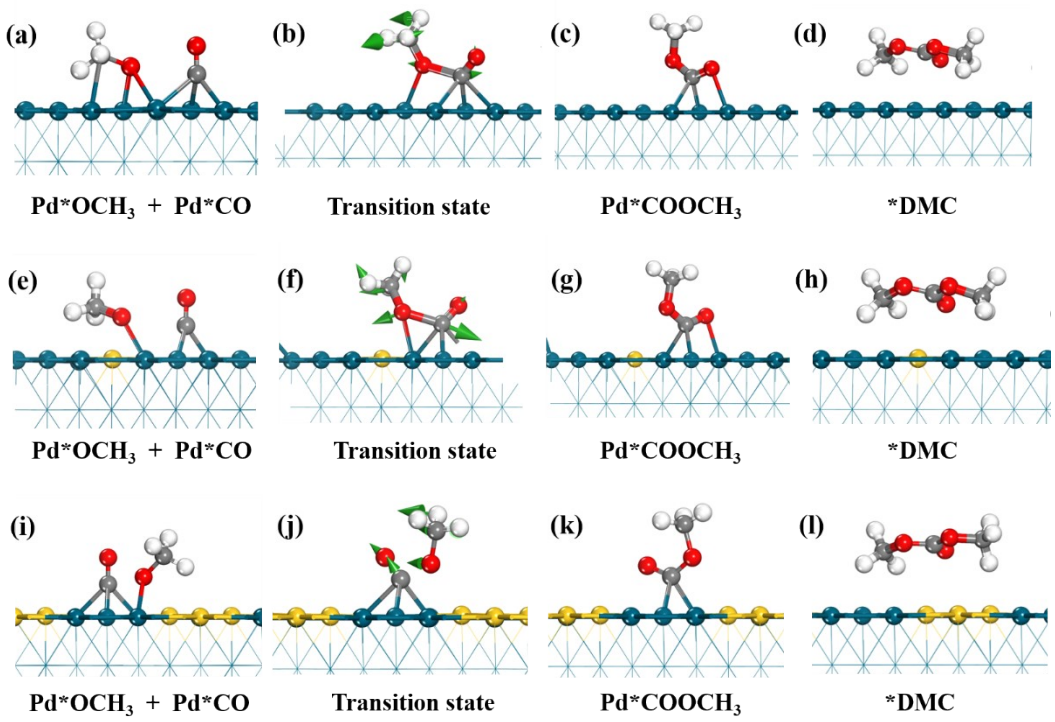

Figure S21. (a-d) Key reaction intermediates on Pd(111). The green arrows represent the direction of vibration of transition state. (e-h) Key reaction intermediates on AuPd-0.03. The green arrows represent the direction of vibration of transition state. (i-l) Key reaction intermediates on AuPd-0.08-cluster. The green arrows represent the direction of vibration of transition state.

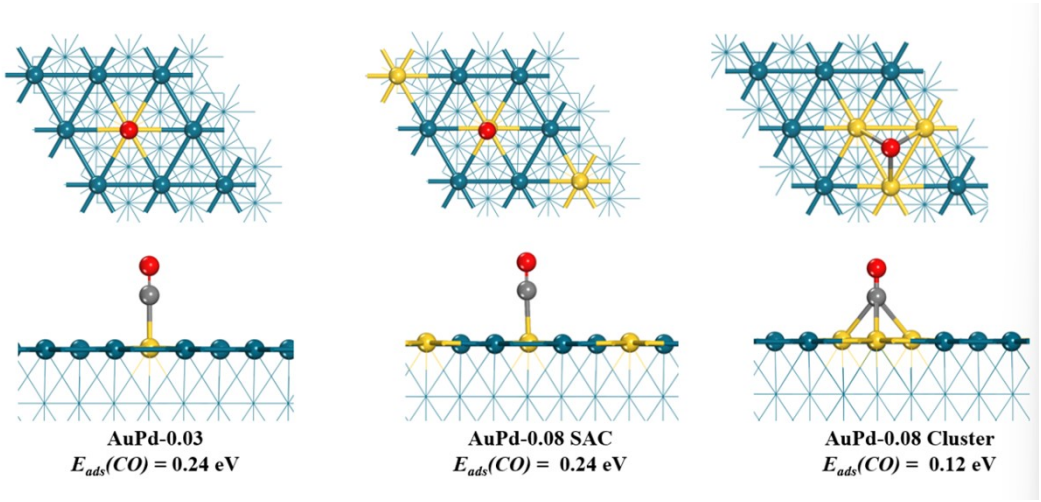

Figure S22. Adsorption energy of CO on the Au site at different models.

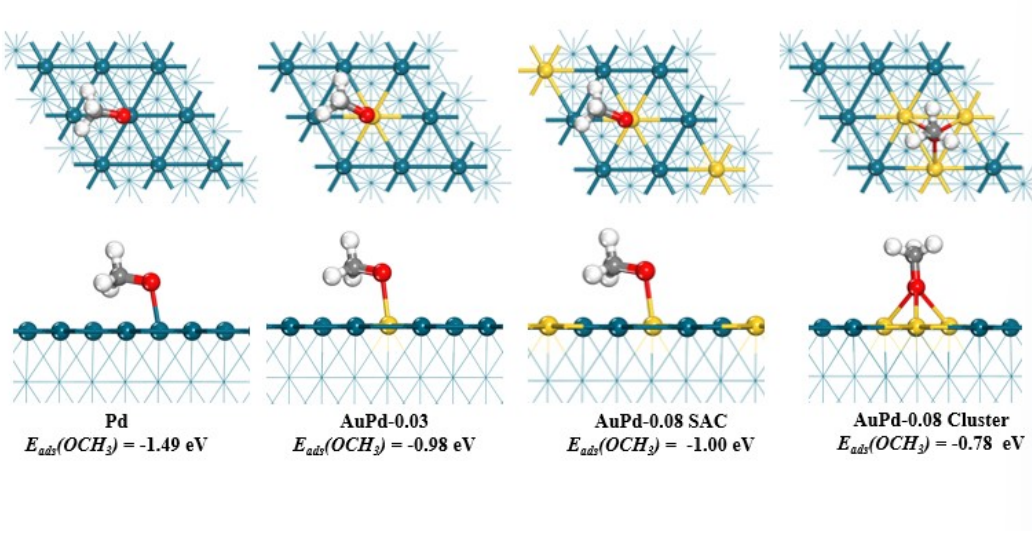

Figure S23. Comparison of adsorption energy of methoxide on the Pd and Au sites at different models.

Table S1 ICP-MS testing of Au content in AuPd-0.08.

Test elements	Sampling quantity（g)	Constant volume V_0（mL)	Dilution ratio f	Element concentration in solution C_1（g/kg)	Au:Pd
Au	0.0353	25	50	156.905	0.1

Table S2 Comparison of XPS before and after AuPd-0.08 electrolysis.

	Name	Start BE	Peak BE	End BE	Atomic %	Au:Pd
Before electrolysis	Au4f	92.5	83.6	80.92	1.72	0.083
	Pd3d	345.5	335.69	331.5	20.77	
After electrolysis	Au4f	92	84.11	81	1.12	0.095
	Pd3d	345	335.78	332.07	11.7	

Table S3. Au L_3-edge EXAFS fitting results. ($S0^2$=0.9)

Sample	Path	*N*	*R*/Å	$\sigma^2/10^{-3}$ Å^2	ΔE_0/eV	R-factor
AuPd-0.08	Pd-Au	8.7±0.9	2.77±0.01	7.49±0.49	6.14±0.83	0.011
	Au-Au	0.3±0.2	2.82±0.01	6.69±0.68		
Au foil	Au-Au	12	2.86±0.01	8.22±0.33	4.44±0.33	0.0035

N is the coordination number.

R is the distance between absorber and backscatter atoms.

σ^2 is the Debye Waller factor.

R-factor is residual factor.

Data ranges:3.0＜k≤12.5 Å^{-1}, 1.0＜R≤3.0Å. ΔE_0 was refined as a global fit parameter.

The number of variable parameters is 4, out of a total of 11.4(Pd) and 11.8(Au) independent points.

Table S4 Performance comparison of electrosynthesis DMC.

Catalyst	Electrosynthesis method	j(mA cm^{-2})	FE(%) or Yield	Reference
AuPd-0.08	Coupling of CO_2 and CH_3OH at single cathode	30	52.3% ~296 umol.$cm^{-2}.h^{-1}$	This work
Pd-B	Coupling of CO_2 and CH_3OH at single cathode	30	47.5%	Chem. Eng. J. **2024**, 498, 155109.
Ni SAs/OMMNC+Pd/C	Coupling of CO_2 and CH_3OH at cathode with Pd/C	12	80%	Energy Environ. Sci., 2023,16, 502-512
Co-CPY/CNTs,	Coupling of CO_2 and CH_3OH at cathode with Pd/C	16	~35 umol.$cm^{-2}.h^{-1}$	Chem. Eng. J. 2024, 486, 150179
NiPc-azo-H2Pp@CNTs	Coupling of CO_2 and CH_3OH at cathode with Pd/C	30	6.21 mmol $L^{-1}h^{-1}$	Adv. Energy Mater. 2024, 14, 2401314
Au+Pd/C	Coupling of CO_2 and CH_3OH at cathode with Pd/C	12	55%	Nature Energy volume 6, pages733–741 (2021)
Au/carbon	electrosynthesis from CO at the anode	11	35%	J. Phys. Chem. B 2005,109, 9140.
$HAuCl_4$/AC	electrosynthesis from CO at the anode	2.4	5.1%	J. Am. Chem. Soc. 2004, 126, 5346.
Copper carbonyl	electrosynthesis from CO at the anode	4	6%	ACS Catal. 2018, 9,859.
$CuCl_2$/graphite	electrosynthesis from CO at the anode	4.6	14.5%	J. Electrochem. Soc.1995, 142, 130.
$PdCl_2$/graphite	electrosynthesis from CO at the anode	5	60%	Chem. Lett. 2002, 31,448.
Pd_3Cu	electrosynthesis from CO at the anode	2.1	93%	Angew. Chem. Int. Ed. 2024, e202401311.

Table S5 Dissolution test of Pd and Au in the electrolyte using ICP-MS

Test Elements	Actual sampling quantity（ml)	Constant volume V0（mL)	Test Element Concentration C_o（ug/L)	Dilution ratio f	Element concentration in solution C_1（ug/L)
Pd	1	10	20.036	1	20.04
Au	1	10	2.498	1	2.5

Table S6 Comparison of electrosynthesis properties of different anode materials

Anode	FE_{MF}(%)	FE_{DMC}(%)
Carbon paper	**1.9**	**52.3**
Carbon felt	13.7	42.5
Carbon glass	20.3	47.5
Carbon paper+IrO_2	32.4	33.5

Table S7 Controlling Different Variables for DMC Electrosynthesis.

Cathode	Electrolyte	Atmosphere	FE_{DMC}
Ni-N-C	0.1M NaBr	CO_2	0
Pd NPs	0.1M $NaBF_4$	CO_2	0
Pd NPs	0.1M NaBr	N_2	0